Journal of Chemistry and Technologies, 2025, *33*(3), 990-999

Journal of Chemistry and Technologies

pISSN 2663-2934 (Print), ISSN 2663-2942 (Online).

journal homepage: http://chemistry.dnu.dp.ua
editorial e-mail: chem.dnu@gmail.com

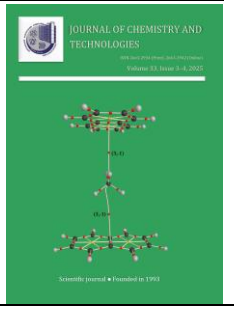

UDC 541.49 + 546.562 + 547.772 + 539.26 + 543.57

SYNTHESIS, X-RAY CRYSTAL STRUCTURE, SPECTROSCOPIC CHARACTERIZATION AND MALDI MASS SPECTRA, HIRSHFELD SURFACE ANALYSIS OF OCTANUCLEAR AZAMETALLACROWN COPPER(II) COMPLEX WITH 3,5-DIMETHYL-1H-PYRAZOLE, OBTAINED BY OXIDATIVE DISSOLUTION METHOD

Yuliya M. Davydenko*, Oleksandr S. Vynohradov, Vadim O. Pavlenko, Igor O. Fritsky
Department of Chemistry, Taras Shevchenko National University of Kyiv, Hetman Pavlo Skoropadsky St, 12, 01033 Kyiv, Ukraine
Received 5 July 2025; accepted 2 October 2025; available online 25 December 2025

Abstract

A novel copper(II) polynuclear complex with deprotonated 3,5-dimethyl-1H-pyrazole of composition $Cu_8(\mu_3\text{-}O)_2(DMPZ\text{-}H)_8(NCO)_2(OAc)_2\cdot 2CH_3OH$ has been synthesized and isolated in the crystalline state. A variety of techniques were employed to identify and characterize the structure of the complex, including IR spectroscopy, microanalysis, MALDI analysis, and single-crystal X-ray diffraction. It was observed that $Cu_8(\mu_3\text{-}O)_2(DMPZ\text{-}H)_8(NCO)_2(OAc)_2\cdot 2CH_3OH$ had been formed as a result of a multistage process of oxidative dissolution of metallic copper with the participation of air oxygen and ammonium ions. This process results in the accumulation of a sufficient concentration of Cu^{2+} ions in the solution, which contributes to both the formation of the final product and the dissolution of metallic copper through the intermediate generation of Cu^{+} species. These intermediates are subsequently oxidized by atmospheric oxygen to yield divalent copper compounds. The resulting octanuclear complex $Cu_8(\mu_3\text{-}O)_2(DMPZ\text{-}H)_8(NCO)_2(OAc)_2\cdot 2CH_3OH$ is a new inverted 24-azametallocrown-8, due to the implementation of the cyclic interaction $(\text{-}Cu\text{-}N\text{-}N\text{-})_8$ formed by eight copper ions and eight μ_2-bridge coordinated 3,5-dimethyl-1H-pyrazole anions. A crystallographic 2-fold axis bisects the obtained octanuclear complex on the same two trinuclear fragments Cu2-Cu3-Cu4^{i} and Cu2^{i}-Cu3^{i}-Cu4, which are sequentially linked by deprotonated bidentate-bridging coordinated molecules of 3,5-dimethyl-1H-pyrazoles and bridging $\mu_3\text{-}O^{2-}$, which are the centers of coordination for three copper cations. Tetradentate-bridged cyanate groups additionally assemble the thrinuclear fragments into an octanuclear complex. Hirshfeld surface analysis, complemented by two-dimensional fingerprint plots, was carried out to investigate the intermolecular interactions in the crystal structure. The results revealed dominant H···H contacts (71.7 %) along with notable contributions from H···C/C···H, H···O/O···H and H···N/N···H interactions, confirming that hydrogen bonding plays a significant role in stabilizing the crystal packing.

Keywords: pyrazole ligands; copper complexes; oxidative dissolution; X-ray crystallography; metallacrown; Hirshfeld surface analysis.

СИНТЕЗ, РЕНТГЕНОСТРУКТУРНИЙ АНАЛІЗ, СПЕКТРАЛЬНА ХАРАКТЕРИСТИКА ТА MALDI МАС-СПЕКТРИ, АНАЛІЗ ПОВЕРХНІ ХІРШФЕЛЬДА ОКТАЯДЕРНОГО КОМПЛЕКСУ КУПРУМУ(II) АЗАМЕТАЛОКРАУНОВОГО ТИПУ З 3,5-ДИМЕТИЛ-1Н-ПІРАЗОЛОМ, ОТРИМАНОГО МЕТОДОМ ОКИСНОГО РОЗЧИНЕННЯ

Юлія М. Давиденко, Олександр С. Виноградов, Вадим О. Павленко, Ігор О. Фрицький
Київський національний університет імені Тараса Шевченка, вул. Гетьмана Павла Скоропадського, 12, 01033 Київ, Україна

Анотація

Піразоли є цінними прекурсорами для синтезу численних сполук завдяки своїй значній біологічній та фармакологічній активності, зокрема антибактеріальній, протигрибковій, протизапальній, протипухлинній, протираковій, антидепресивній, антиоксидантній та противірусній діям. У даній роботі представлено кристалічну структуру нової сполуки, яка містить піразольне кільце в молекулярному каркасі. А саме, синтезований та виділений в кристалічному стані новий поліядерний комплекс купруму(II) з депротонованим 3,5-диметилпіразолом складу $Cu_8(\mu_3\text{-}O)_2(DMPZ\text{-}H)_8(NCO)_2(OAc)_2\cdot 2CH_3OH$. Для ідентифікації та характеристики структури комплексу використовували ІЧ-спектроскопію, елементний аналіз, MALDI мас-спектрометрію та рентгеноструктурний аналіз. Встановлено, що $Cu_8(\mu_3\text{-}O)_2(DMPZ\text{-}H)_8(NCO)_2(OAc)_2\cdot 2CH_3OH$ утворюється в результаті багатостадійного процесу окиснювального розчинення металічної міді за участю кисню повітря та іонів амонію. Такий процес приводить до накопичення в розчині достатньої концентрації іонів Cu^{2+}, що сприяє як утворенню кінцевого продукту, так і розчиненню металічної міді через проміжну генерацію сполук Cu^{+}. Проміжні сполуки Cu^{+} окиснюються атмосферним киснем з утворенням сполук Cu^{2+} з подальшим

**Corresponding author: email: davydenko300808@gmail.com*

Journal of Chemistry and Technologies, 2025, *33*(3), 990-999

формуванням восьмиядерного комплексу азаметалокраунового типу складу $Cu_8(\mu_3\text{-}O)_2(DMPZ\text{-}H)_8(NCO)_2(OAc)_2\cdot 2CH_3OH$. Отриманий восьмиядерний комплекс є інвертованим азаметалокрауном (24-азаметалокраун-8) внаслідок реалізації циклічної взаємодії $(\text{-}Cu\text{-}N\text{-}N\text{-})_8$ завдяки послідовному поєднанню восьми атомів купруму містково координованими молекулами ліганду 3,5-диметил-1Н-піразолу. Кристалографічна ось другого порядку розділяє отриманий восьмиядерний комплекс на два однакові триядерні фрагменти Cu2-Cu3-Cu4^i та Cu2^i-Cu3^i-Cu4, які послідовно з'єднані бідентатно-містково координованими молекулами 3,5-диметил-1Н-піразолу та містками $\mu_3\text{-}O^{2-}$, які є центрами координації для трьох катіонів купруму. Триядерні фрагменти додатково з'єднані тетрадентатно-містковими ціанатними групами в кінцевий восьмиядерний комплекс. Для дослідження міжмолекулярних взаємодій у кристалічній структурі комплексу було проведено аналіз поверхні Хіршфельда, доповнений двовимірними графіками відбитків. Результати показали домінуючі контакти H···H (71.7 %) разом із помітним внеском взаємодій H···C/C···H, H···O/O···H та H···N/N···H, що підтверджує, що водневі зв'язки відіграють значну роль у стабілізації кристалічної упаковки отриманого комплексу.

Ключові слова: піразольні ліганди; комплекси купруму; кристалічна структура; окисне розчинення; металокрауни; аналіз поверхні Хіршфельда.

Introduction

Pyrazole derivatives represent a group of heterocyclic compounds defined by a five-membered ring containing two adjacent nitrogen atoms. They have attracted considerable interest in medicinal chemistry owing to their wide range of biological activities and therapeutic prospects. These compounds demonstrate various pharmacological effects, including antimicrobial, anti-inflammatory, anticancer, antioxidant, antiviral, antidiabetic, and neuroprotective properties [1–5]. The remarkable medicinal potential of pyrazole can be demonstrated by the range of marketed drugs containing this moiety, including Celecoxib [6], Lonazolac [7], Mepirizole [8], Rimonabant [9], Acomplia [10], Cimetidine [11], Fipronil [12], Dexacoxib [13], among others. Copper is among the most abundant and less toxic transition metals. Its natural bioavailability and versatile redox properties are utilized by living systems to perform oxygenase and oxidase reactions using O_2 or H_2O_2 as oxidants. Drawing inspiration from the activity of Cu-containing metalloenzymes, researchers have designed synthetic methodologies for organic transformations under environmentally friendly conditions. Moreover, copper can catalyze a variety of reactions typically associated with 4d and 5d metals, such as palladium (Pd), platinum (Pt), and rhodium (Rh), including nitrogen insertions and C–C or C–heteroatom coupling processes [14].

Over the past several decades, copper pyrazolate complexes have garnered significant attention due to their structural versatility and promising applications in magnetism [15–18], luminescence [19], and catalysis [20–22]. The pyrazolate anion readily coordinates to copper ions through an N,N′-bridging mode. These complexes exhibit a wide range of structural diversity, including di-, tri-, tetra-, penta-, hexa-, and polynuclear architectures, as well as chain, layered, and three-dimensional network formations [23–27].

We are interested in the self-assembly of novel polynuclear metal complexes employing pyrazole and both cyanate and carboxylate as bridging ligands. It has been long known that coordination compounds may be obtained starting from elemental metals. This synthetic strategy, known as the oxidative dissolution method or direct synthesis of coordination compounds, was used to prepare numerous homo- and heterobimetallic, both mononuclear and polynuclear complexes, with different aminoalcohol ligands such as diethanolamine and others (HL) [28]. Here, we report the synthesis and crystal structure of new undecanuclear $Cu_8(\mu_3\text{-}O)_2(DMPZ\text{-}H)_8(NCO)_2(OAc)_2\cdot 2CH_3OH$ (DMPZ = 3,5-dimethyl-1H-pyrazole). The compound was prepared starting from copper metal, ammonium acetate, sodium cyanate and pyrazole ligand (DMPZ) in a dimethylformamide solution under ambient air and water conditions. We are interested in understanding how the presence of both cyanate and carboxylate as bridging ligands can influence the structure and properties of the obtained complexes.

Hirshfeld surface analysis was also done to obtain more detailed information about the structure of undecanuclear complex $Cu_8(\mu_3\text{-}O)_2(DMPZ\text{-}H)_8(NCO)_2(OAc)_2\cdot 2CH_3OH$.

Experimental and methods

All chemical reagents were commercial products of reagent grade and used without further purification unless otherwise specified.

IR spectroscopy. IR spectra were recorded with a Perkin-Elmer Spectrum BX FT-IR in the range of 400–4000 cm^{-1} in KBr pellets.

Elemental analysis. The elemental (CHN) analysis was performed using a CHNOS analyzer vario MICRO cube Elementar. The result was reported as the percentage by weight of each element, with a precision of ±0.30 %.

MALDI mass spectrometry. Positive and negative MALDI mass spectra of the complex were recorded on an Autoflex II (Bruker Daltonics Inc.). Solutions for MALDI mass spectrometry were prepared using reagent grade dimethylformamide and the obtained data (masses and intensities) were compared to those calculated by using the IsoPro isotopic abundance simulator, version 2.1 [29]. Peaks containing copper (II) ions are identified as the centres of isotopic clusters.

Crystal structure determination. Crystal data, data collection and structure refinement details are summarized in Table 1. The structure was solved using a set of programs *CrysAlis PRO* 1.171.43.144a (Rigaku OD, 2024), SHELXT 2018/2 (Sheldrick, 2018), *SHELXL* 2018/3 (Sheldrick, 2015), Olex2 1.5-ac6-020 (Dolomanov *et al.*, 2009) [30]. The structure of the title compound was deposited at the Cambridge Crystallographic Data Centre (№2469927)[31].

Table 1

Crystallographic data, details of data collection, and characteristics of data refinement for the obtained complex

Chemical formula	$C_{46}H_{62}Cu_8N_{18}O_8 \cdot 2(HO) \cdot 2(CH_3)$
M_r	1567.54
Crystal system, space group	Monoclinic, $P2_1/n$
Temperature (K)	293
a, b, c (Å)	7.5053 (3), 32.6038 (9), 13.1647 (5)
β (°)	95.739 (4)
V (Å^3)	3205.3 (2)
Z	2
μ (mm^{-1})	2.67
Crystal size (mm)	0.12 × 0.07 × 0.03
Data collection	
Diffractometer	XtaLAB Synergy, Dualflex, HyPix
Absorption correction	Multi-scan *CrysAlis RED*, Oxford Diffraction Ltd., Version 1.171.31.8 (release 12-01-2007 CrysAlis171 .NET) (compiled Jan 12 2007,17:49:11) Empirical absorption correction using spherical harmonics, implemented in SCALE3 ABSPACK scaling algorithm.
T_{min}, T_{max}	0.637, 1.000
No. of measured, independent and observed [$I > 2\sigma(I)$] reflections	43316, 8072, 4444
R_{int}	0.059
$(\sin \theta/\lambda)_{max}$ (Å^{-1})	0.680
Refinement	
$R[F^2 > 2\sigma(F^2)]$, $wR(F^2)$, S	0.064, 0.182, 1.02
No. of reflections	8072
No. of parameters	383
H-atom treatment	H-atom parameters constrained
$\Delta\rho_{max}$, $\Delta\rho_{min}$, e Å^{-3}	1.82, -0.58

Synthesis of polynuclear complex. Complex $Cu_8(\mu_3\text{-}O)_2(DMPZ\text{-}H)_8(NCO)_2(OAc)_2 \cdot 2CH_3OH$ was synthesized using the oxidative dissolution method under free access of air oxygen. A mixture of 3,5-dimethyl-1H-pyrazole (0.96 g; 0.01 mol), ammonium acetate (0.77 g; 0.01 mol), and sodium cyanate (0.65 g; 0.01 mol) in 20 mL of dimethylformamide (DMF) solution was magnetically stirred with copper powder (0.64 g; 0.01 mol) at room temperature until the solid was completely dissolved. The resulting green solution was filtered, and the filtrate was left to stand at room temperature in the air for 2 days. The green needle-shaped crystals of the title compound, suitable for X-ray analysis, were salting out with methanol vapors within 2 days. Yield 38 %. Elemental analysis (%): calculated C, 36.65; H, 4.12; N, 16.73. Found: C, 36.61; H, 4.08; N, 16.33.

The synthesis of 3,5-dimethyl-1H-pyrazole was carried out according to the following method [26].

Results and discussion

Copper powder, ammonium acetate, sodium cyanate, and DMPZ were taken at a 1 : 1 : 1 : 1 molar ratio in DMF. All reactions were initiated and brought to completion by heating and stirring. Green solutions were obtained at the end of the reactions that afforded crystals of the polynuclear

compound directly after filtration. The formation of $Cu_8(\mu_3\text{-}O)_2(DMPZ\text{-}H)_8(NCO)_2(OAc)_2\cdot 2CH_3OH$ can be described by the following reaction scheme:

$$Cu^0 + DMPZ + NH_4COOCH_3 + NaNCO + DMF/CH_3OH + O_2 \rightarrow$$
$$\rightarrow Cu_8(\mu_3\text{-}O)_2(DMPZ\text{-}H)_8(NCO)_2(OAc)_2\cdot 2CH_3OH + NH_3 + H_2O + NaCOOCH_3$$

Infrared spectra. The stretching vibrations of the pyrazole ligands, namely ν(N–H) and ν(C–H, aliphatic) appear as multiple bands in the region of 2880–3100 cm^{-1}. The other absorption peaks of the pyrazole ligands appear at 1700–650 cm^{-1}. Weak bands corresponding to the acetate methyl groups C–H stretching vibrations are identified at 2800–2900 cm^{-1}.

The IR spectrum of the title compound displays several main bands: 3100 m, 2930 m, 2890 m, 2140 m, 1670 s, 1615 m, 1590 s, 1430 m, 1350 m, 1150 w, 1100 w, 1050 m, 980 w, 770 w, 620 m, 490 m cm^{-1}. The carboxylate groups of the acetate ions give rise to two strong bands in the spectrum of **2**: an asymmetric stretching band at 1560 cm^{-1} and a symmetric stretching band at 1440 cm^{-1}. The difference in wavenumbers, Δ=120 cm^{-1}, between the antisymmetric and symmetric COO^- stretching frequencies indicates the presence of bridging or chelating acetate ligands [32], which is consistent with the X-ray structure determination.

The bands observed in the range of double bonds 2140 cm^{-1} suggest characteristic vibration bands of the NCO group in the structure, which in the compound exhibits a rather rare method of coordination - tetradentate-bridging (μ_4-NCO). Only one example of such an unusual coordination of the cyanate group has been found in the literature [33]. The medium intensity bands at 1615 cm^{-1} and 1050 cm^{-1} may be attributed to the C=C or C=N groups of the pyrazole ligand, and the second absorption band belongs to C-N groups, respectively.

MALDI mass spectrum. In the MALDI mass spectrum of the dimethylformamide solution of the obtained octanuclear complex, isotopic patterns from mononuclear particles with signal profiles characteristic of the copper isotopic distribution can be distinguished (Fig. 1). This indicates the destruction of complex particles under the influence of laser radiation (Fig. 1). The isotopic patterns and their mass spectrometric characteristics detected in the mass spectrum are given in Table 2.

Table 2

Mass spectrometric characteristics of copper particles in the MALDI-MS spectrum of the obtained complex $Cu_8(\mu_3\text{-}O)_2(DMPZ\text{-}H)_8(NCO)_2(OAc)_2\cdot 2CH_3OH$

Pattern	m/z	$M_{calc.}$
$[Cu(DMPZ\text{-}H)_2(DMPZ)$ ДМФА + $H^+]^+$	423.882	423
$[Cu(DMPZ\text{-}H)_2(DMPZ)$ 2ДМФА + $3H^+]^+$	499.043	499
$[Cu(DMPZ\text{-}H)_2(DMPZ)_2$ (OAc) + $Na^+]^+$	527.043	527

Description of the complex. The crystal structure determination reveals that $Cu_8(\mu_3\text{-}O)_2(DMPZ\text{-}H)_8(NCO)_2(OAc)_2\cdot 2CH_3OH$ (Fig. 2) is an octanuclear compound with an unexpected molecular topology. Based on the classification of metallacrowns [34], complex $Cu_8(\mu_3\text{-}O)_2(DMPZ\text{-}H)_8(NCO)_2(OAc)_2\cdot 2CH_3OH$ can be considered as a new inverted 24-azametallocrown-8, due to the implementation of the cyclic interaction $(\text{-}Cu\text{-}N\text{-}N\text{-})_8$ formed by eight copper ions and eight μ_2-bridge coordinated DMPZ anions. The title compound is constructed from $Cu2\text{-}Cu3\text{-}Cu4^i$ and $Cu2^i\text{-}Cu3^i\text{-}Cu4$ fragments by sequentially linking deprotonated bidentate-bridging coordinated molecules of 3,5-dimethyl-1H-pyrazoles and bridging $\mu_3\text{-}O^{2-}$, which are the centers of coordination for three copper cations. The trinuclear fragments are additionally assembled by tetradentate-bridged cyanate groups and two copper atoms Cu1, $Cu1^i$ into an eight-nuclear complex. The terminal positions of two copper atoms Cu3, $Cu3^i$ are occupied by bidentate-bridged acetate anion molecules (Fig. 2). A crystallographic 2-fold axis running through Cu1 and $Cu1^i$ bisects the obtained complex in such a way that the trinuclear fragments $Cu2\text{-}Cu3\text{-}Cu4^i$ and $Cu2^i\text{-}Cu3^i\text{-}Cu4$ are similar. The trinuclear $Cu2\text{-}Cu3\text{-}Cu4^i$ fragment of the title complex is located at the center of a ten-membered Cu3N5OC cycle formed from two bidentate-bridging coordinated 3,5-dimethyl-1H-pyrazole molecules that bind the Cu2-Cu3 and $Cu3\text{-}Cu4^i$ copper atoms to each other and the μ_4-NCO anion (combining Cu2 and $Cu4^i$).

Journal of Chemistry and Technologies, 2025, *33*(3), 990-999

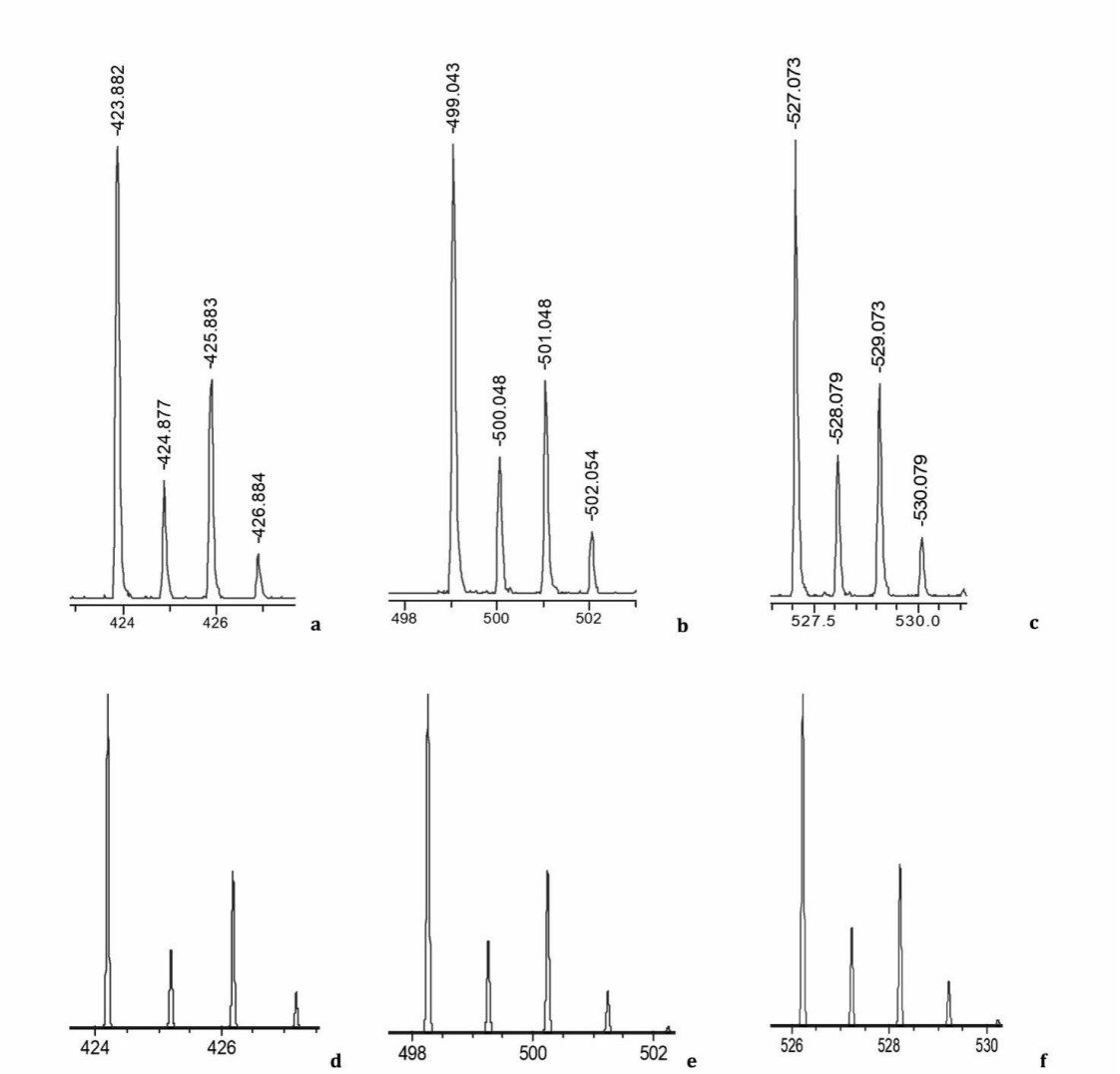

Fig. 1. Isotopic patterns in MALDI mass spectra of compound $Cu_8(\mu_3\text{-}O)_2(DMPZ\text{-}H)_8(NCO)_2(OAc)_2\cdot 2CH_3OH$ for particles of $[Cu(DMPZ\text{-}H)_2(DMPZ)\cdot DMFA + H^+]^+$ observed (a) and calculated (d); $[Cu(DMPZ\text{-}H)_2(DMPZ)\cdot 2DMFA + 3H^+]^+$ observed (b) and calculated (e); $[Cu(DMPZ\text{-}H)_2(DMPZ)_2(OAc) + Na^+]^+$ observed (c) and calculated (f)

The center of organization of the three copper atoms in the cycle is the $\mu_3\text{-}O^{2-}$ group, which in turn is linked by a hydrogen bond to the CH_3OH molecule. The O-atom is 0.593 Å out of the Cu_3-plane in the trinuclear unit. The trinuclear fragment of the complex, the apparent plane of which is formed of three copper atoms Cu2-Cu3-$Cu4^i$, resembles an isosceles triangle with almost equal sides Cu2-Cu3 3.233 Å and Cu4i-Cu3 3.184 Å, and the foundation of this triangle is its apparent side Cu2-$Cu4^i$ with a length of 3.602 Å. The value of the Cu2-Cu3-$Cu4^i$ angle is 68.32° (Table 3). The $Cu3^i$ and Cu3 copper atoms are in a distorted square pyramidal environment (N2O2 + O). This is confirmed by the values of geometry indices $\tau_5 \approx 0.0545$ [35] (Table 4). Thus, in the equatorial plane of copper atoms, there are two nitrogen atoms from deprotonated bidentate-bridging coordinated molecules of 3,5-dimethyl-1H-pyrazole (Cu-N 1.915(2)–1.925(2) Å), one oxygen atom from $\mu_3\text{-}O^{2-}$(Cu-O 2.035(0) Å) and another oxygen atom from the bidentate-chelate coordinated acetate anion (Cu-O 1.972(0) Å). This type of coordination of the acetate group in copper (II) complexes always leads to a different spatial arrangement of the Cu-O bonds, so its other bond occupies the axial position of the square pyramid (Cu-O 2.410(1) Å). Notably, Cu1, $Cu1^i$, Cu2, $Cu2^i$ (N3O) and Cu4, $Cu4^i$ (N2O2) copper atoms have a four-coordinate environment. According to this, the parameters τ_4 and τ_4' were calculated and found to have values (Table 4) indicating a seesaw geometry [36]. The Cu···Cu intramolecular separations in all trinuclear metallacycles are within the range of 3.184(0) - 3.602(1) Å (Table 3).

Table 3

Selected bond lengths (Å) and bond angles (°) for the title complex $Cu_8(\mu_3\text{-}O)_2(DMPZ\text{-}H)_8(NCO)_2(OAc)_2\cdot 2CH_3OH$, (-*x*, -*y*, -*z*+1)

Cu1—N5	1.936 (5)	Cu3—N1	1.916 (5)
Cu1—N4	1.937 (5)	Cu3—N8	1.932 (5)
Cu1—O1	1.937 (5)	Cu3—O4	1.977 (5)
Cu1—N9^{i}	1.945 (5)	Cu3—O2	2.035 (4)
Cu2—N7	1.924 (5)	Cu3—O3	2.420 (6)
Cu2—N6	1.933 (6)	Cu4—N2^{i}	1.925 (5)
Cu2—N9^{i}	1.990 (5)	Cu4—N3	1.946 (5)
Cu2—O2	2.024 (4)	Cu4—O1	1.975 (5)
N5—Cu1—N4	108.5 (2)	O4—Cu3—O2	150.6 (2)
N5—Cu1—O1	137.0 (2)	N1—Cu3—O3	103.0 (2)
N4—Cu1—O1	90.6 (2)	N8—Cu3—O3	104.0 (2)
N5—Cu1—N9^{i}	90.8 (2)	O4—Cu3—O3	57.5 (2)
N4—Cu1—N9^{i}	137.7 (3)	O2—Cu3—O3	93.0 (2)
O1—Cu1—N9^{i}	100.5 (2)	N1—Cu3—C22	101.2 (3)
N7—Cu2—N6	98.7 (2)	N8—Cu3—C22	101.2 (3)
N7—Cu2—N9^{i}	154.5 (2)	O4—Cu3—C22	28.5 (2)
N6—Cu2—N9^{i}	89.1 (2)	O2—Cu3—C22	122.1 (3)
N7—Cu2—O2	88.79 (19)	O3—Cu3—C22	29.1 (2)
N6—Cu2—O2	162.7 (2)	N2^{i}—Cu4—N3	100.0 (2)
N9^{i}—Cu2—O2	90.73 (19)	N2^{i}—Cu4—O1	153.0 (3)
N1—Cu3—N8	152.9 (2)	N3—Cu4—O1	89.6 (2)
N1—Cu3—O4	95.7 (2)	N2^{i}—Cu4—O2^{i}	89.4 (2)
N8—Cu3—O4	96.6 (2)	N3—Cu4—O2^{i}	157.0 (2)
N1—Cu3—O2	89.47 (18)	O1—Cu4—O2^{i}	91.31 (19)
N8—Cu3—O2	91.57 (18)		
Cu1—O1—Cu4	116.8 (3)	Cu4^{i}—O2—Cu3	103.49 (17)
Cu4^{i}—O2—Cu2	125.88 (19)	Cu2—O2—Cu3	105.38 (18)
Cu1^{i}—N9—Cu2^{i}	116.6 (3)	C24—O5—H5O	116.4

Table 4

Geometry index and donor environment of the central atoms in the title complex $Cu_8(\mu_3\text{-}O)_2(DMPZ\text{-}H)_8(NCO)_2(OAc)_2\cdot 2CH_3OH$, (-*x*, -*y*, -*z*+1)

Central atom	Donor environment	Geometry index		
		τ_5	τ_4	τ_4'
Cu1	N3O	-	0.6	0.59
Cu1^{i}	N3O	-	0.6	0.59
Cu2	N3O	-	0.35	0.28
Cu2^{i}	N3O	-	0.35	0.28
Cu3	N2O2 + O	0.0545	-	-
Cu3^{i}	N2O2 + O	0.0545	-	-
Cu4	N2O2	-	0.35	0.35
Cu4^{i}	N2O2	-	0.35	0.35

The Hirshfeld surface analysis and the associated two-dimensional fingerprint plots were performed using Crystal Explorer 21.5 software [37], with a standard resolution of the three-dimensional d_{norm} surfaces plotted over a fixed colour scale of –0.5177 (red) to 1.4919 (blue) a.u. There are 12 red spots on the d_{norm} surface. The dark-red spots arise as a result of short interatomic contacts and represent negative d_{norm} values on the surface, while the other weaker intermolecular interactions appear as light-red spots. The Hirshfeld surfaces mapped over d_{norm} are shown for the H···H, H···C/C···H, H···O/O···H and H···N/N···H contacts (Fig. 3), the overall two-dimensional fingerprint plot and the decomposed two-dimensional fingerprint plots are given in Fig. 4. The shortest intermolecular contacts are two H···O interactions of 1.938 Å. These correspond to the hydrogen bonds O5–H5O···O2^{i} between the complex molecule and the solvate methanol molecule.

Journal of Chemistry and Technologies, 2025, *33*(3), 990-999

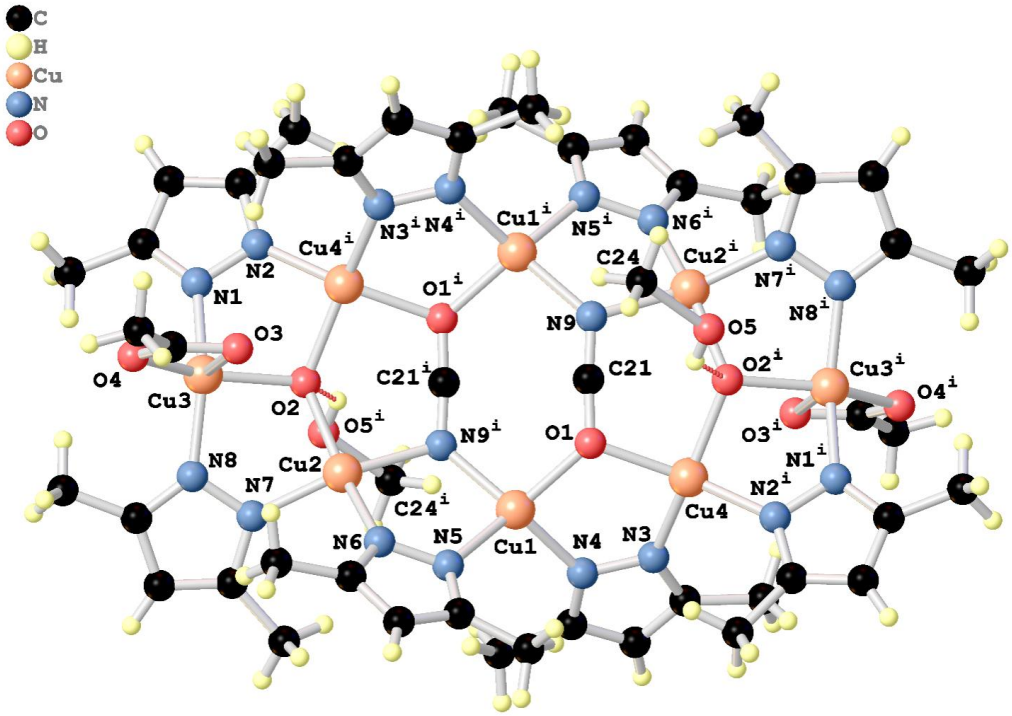

Fig. 2. The molecular structure of the title compound $Cu_8(\mu_3\text{-}O)_2(DMPZ\text{-}H)_8(NCO)_2(OAc)_2\cdot 2CH_3OH$, (-*x*, -*y*, -*z*+1)

The most significant contributions to the overall crystal packing are from H···H (71.7 %), H···C/C···H (11.5 %), H···O/O···H (7 %) and H···N/N···H (6.5 %) contacts. There is a small contribution from Cu···H/H···Cu (1.5 %), O···O (1.1%), O···N/N···O (0.4%), Cu···O/O···Cu (0.2%) and C···O/O···C (0.1 %) weak intermolecular contacts. The relative percentage contributions to the overall Hirshfeld surface by elements: H···all atoms – 79.8 %, C···all atoms – 7.6 %, O···all atoms – 5.7 %, N···all atoms – 5.4 % and Cu···all atoms – 1.5 %. Also, quantitative physical properties of the Hirshfeld surface for this compound were obtained, such as molecular volume (1468.13 Å^3), surface area (976.71 Å^2), globularity (0.640), as well as asphericity (0.142). The asphericity value remains relatively low, indicating that the molecular shape is close to isotropic, though with a slightly more pronounced deviation from spherical symmetry compared to more compact molecules. Similarly, the globularity value below one suggests that the molecular surface is somewhat more structured and less compact than a perfect sphere, reflecting a modestly elongated or irregular molecular form.

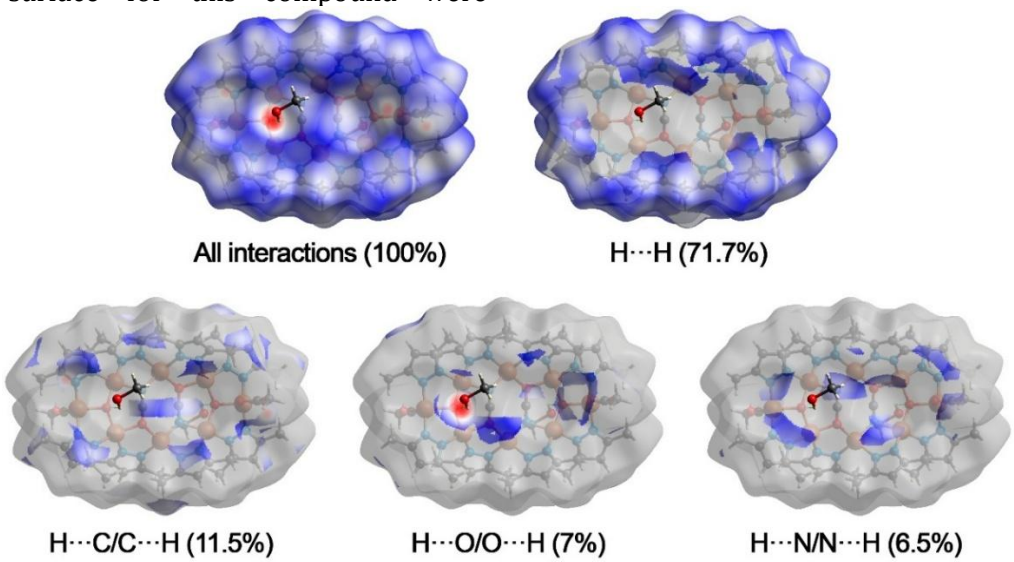

Fig. 3. Projections of Hirshfeld surfaces mapped over normalized contact distance (d_{norm}) illustrating the overall molecular interactions and highlighting individual contact types (H···H, H···C and H···O) in the crystal structure

Journal of Chemistry and Technologies, 2025, *33*(3), 990-999

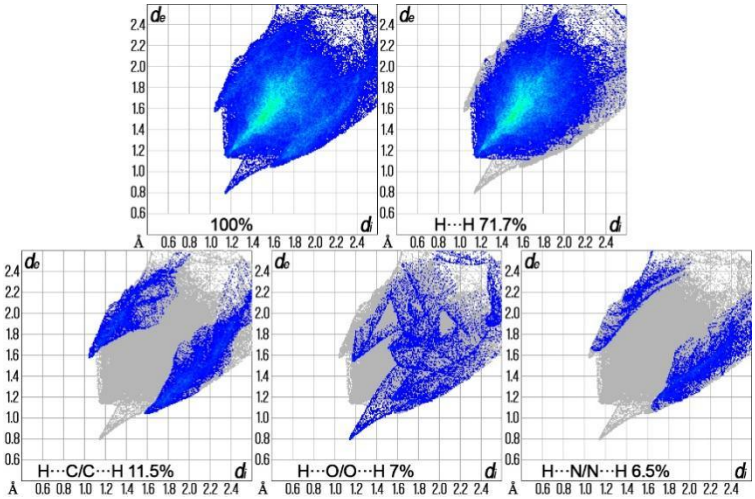

Fig. 4. Overall two-dimensional fingerprint plot and decomposed plots delineated into specified interaction types, corresponding to the Hirshfeld surfaces mapped with the d_{norm} function

Conclusions

In this work, a method of oxidative dissolution was used to obtain an unexpected new octanuclear copper (II) complex $Cu_8(\mu_3\text{-}O)_2(DMPZ\text{-}H)_8(NCO)_2(OAc)_2{\cdot}2CH_3OH$ with 3,5-dimethyl-1H-pyrazole azametallocrown type. Various techniques were used to identify and characterize the structure of complex $Cu_8(\mu_3\text{-}O)_2(DMPZ\text{-}H)_8(NCO)_2(OAc)_2{\cdot}2CH_3OH$, such as IR spectroscopy, microanalyses, MALDI mass spectrometry, and single-crystal X-ray diffraction. It was found that $Cu_8(\mu_3\text{-}O)_2(DMPZ\text{-}H)_8(NCO)_2(OAc)_2{\cdot}2CH_3OH$ had been formed as a result of a multistage process of oxidative dissolution of metallic copper with the participation of air oxygen and ammonium ions. This process leads to the appearance of a sufficient amount of Cu^{2+} ions in the solution, which partially ensures the production of the final compound, as well as the dissolution of zero-valent copper through the formation of intermediate Cu^{1+} compounds, which are oxidized by air oxygen to form divalent copper compounds. It has also been found that ammonium cyanate is formed in parallel through exchange reactions. The resulting octanuclear complex $Cu_8(\mu_3\text{-}O)_2(DMPZ\text{-}H)_8(NCO)_2(OAc)_2{\cdot}2CH_3OH$ is a new inverted 24-azametallocrown-8, due to the implementation of the cyclic interaction $(\text{-Cu-N-N-})_8$ formed by eight copper ions and eight μ_2-bridge coordinated 3,5-dimethyl-1H-pyrazole anions. A crystallographic 2-fold axis running through two copper atoms (Cu1 and $Cu1^i$) bisects the obtained octanuclear complex on the same two trinuclear fragments Cu2-Cu3-$Cu4^i$ and $Cu2^i$-$Cu3^i$-Cu4, which are sequentially linked by deprotonated bidentate-bridging coordinated molecules of 3,5-dimethyl-1H-pyrazoles and bridging $\mu_3\text{-}O^{2-}$, which are the centers of coordination for three copper cations and deals with CH_3OH molecules by hydrogen bonds. The thrinuclear fragments are additionally assembled by tetradentate-bridged cyanate groups and two copper atoms Cu1, $Cu1^i$ into an octanuclear complex. The $Cu3^i$ and Cu3 copper atoms are in a square pyramidal environment (N_2O_2 + O). The values of geometry indices $\tau_5 \approx 0.0545$ confirm this. Accordingly, Cu1, $Cu1^i$, Cu2, $Cu2^i$ (N_3O) and Cu4, $Cu4^i$ (N_2O_2) copper atoms have a four-coordinate environment, since the parameters τ_4 and τ_4' were calculated and indicate a seesaw geometry. The Hirshfeld surface analysis confirmed that intermolecular H···H contacts contribute most significantly to the crystal packing. The calculated shape descriptors, including low asphericity and moderate globularity, suggest a relatively isotropic yet slightly elongated molecular geometry.

Funding information

The work was carried out with financial support from the Ministry of Education and Science of Ukraine within the framework of the project “Molecular Catalysts for Electrochemical Water Splitting Based on Polydentate and Macro(bi)cyclic Compounds of Non-Noble Metals” (project No. RN/61-2024 (24DF037-04H)), funded under the call “Scientific and Scientific-Technical Projects Financed by the External Assistance Instrument of the European Union for the Implementation of Ukraine’s Commitments under the EU Framework Programme for Research and Innovation Horizon 2020.”

Acknowledgements

The authors are grateful to the FAIRE programme provided by the Cambridge Crystallographic Data Centre (CCDC) for the opportunity to use the Cambridge Structural Database (CSD) and associated software. Also, the authors are appreciative to the II European Chemistry School for Ukrainians for providing a comprehensive overview of current trends in European chemical science. https://acmin.agh.edu.pl/en/detail/s/ii-european-chemistry-school-for-ukrainians

References

[1] Yusof, Z., Ramasamy, S., Mahmood, N. Z., Yaacob, J. S. (2018). Vermicompost supplementation improves the stability of bioactive anthocyanin and phenolic compounds in Clinacanthus nutans Lindau. *Molecules, 23*(6), 1345. https://doi.org/10.3390/molecules23061345

[2] Ameziane El Hassani, I., Rouzi, K., Assila, H., Karrouchi, K., Ansar, M. H. (2023). Recent advances in the synthesis of pyrazole derivatives: a review. *Reactions, 4*(3), 478–504. https://doi.org/10.3390/reactions4030029

[3] Ebenezer, O., Shapi, M., Tuszynski, J. A. (2022). A review of the recent development in the synthesis and biological evaluations of pyrazole derivatives. *Biomedicines, 10*(5), 1124. https://doi.org/10.3390/biomedicines10051124

[4] Menezes, R. A., Bhat, K. S. (2025). Synthetic aspects, structural insights and pharmacological potential of pyrazole derivatives: an overview. *Discover Applied Sciences, 7*(2), 137. https://doi.org/10.1007/s42452-025-06528-x

[5] Ansari, A., Ali, A., Asif, M. (2017). Biologically active pyrazole derivatives. *New Journal of Chemistry, 41*(1), 16-41. https://doi.org/10.1039/C6NJ03181A

[6] Abdellatif, K. R., Fadaly, W. A., Elshaier, Y. A., Ali, W. A., Kamel, G. M. (2018). Non-acidic 1, 3, 4-trisubstituted-pyrazole derivatives as lonazolac analogs with promising COX-2 selectivity, anti-inflammatory activity and gastric safety profile. *Bioorganic Chemistry, 77*, 568–578. https://doi.org/10.1016/j.bioorg.2018.02.018

[7] Onoa, G. B., Moreno, V. (2002). Study of the modifications caused by cisplatin, transplatin, and Pd (II) and Pt (II) mepirizole derivatives on pBR322 DNA by atomic force microscopy. *International Journal of Pharmaceutics, 245*(1-2), 55–65. https://doi.org/10.1016/S0378-5173(02)00332-0

[8] Porcu, A., Melis, M., Turecek, R., Ullrich, C., Mocci, I., Bettler, B., Castelli, M. P. (2018). Rimonabant, a potent CB1 cannabinoid receptor antagonist, is a Gαi/o protein inhibitor. *Neuropharmacology, 133*, 107–120. https://doi.org/10.1016/j.neuropharm.2018.01.024

[9] Shi, C., Ma, C., Ma, H., Zhou, X., Cao, J., Fan, Y., Huang, G. (2016). Copper-catalyzed synthesis of 1, 3, 4-trisubstituted and 1, 3, 4, 5-tetrasubstituted pyrazoles via [3+ 2] cycloadditions of hydrazones and nitroolefins. *Tetrahedron, 72*(27-28), 4055–4058. https://doi.org/10.1016/j.tet.2016.05.034

[10] Hughes, A., Hendrickson, R. G., Chen, B. C. C., Valento, M. (2018). Severe loperamide toxicity associated with the use of cimetidine to potentiate the "high". *The American journal of emergency medicine, 36*(8), 1527-e3. https://doi.org/10.1016/j.ajem.2018.05.025

[11] Huang, Q., Tran, G., Pardo, D. G., Tsuchiya, T., Hillebrand, S., Vors, J. P., Cossy, J. (2015). Palladium-catalyzed phosphonylation of pyrazoles substituted by electron-withdrawing groups. *Tetrahedron, 71*(39), 7250–7259. https://doi.org/10.1016/j.tet.2015.03.099

[12] Mullins, K. B., Thomason, J. M., Lunsford, K. V., Pinchuk, L. M., Langston, V. C., Wills, R. W., Mackin, A. J. (2012). Effects of carprofen, meloxicam and deracoxib on platelet function in dogs. *Veterinary Anaesthesia and Analgesia, 39*(2), 206–217. https://doi.org/10.1111/j.1467-2995.2011.00684.x

[13] El-Din, M. M. G., El-Gamal, M. I., Abdel-Maksoud, M. S., Yoo, K. H., Baek, D., Choi, J., Oh, C. H. (2016). Design, synthesis, and in vitro antiproliferative and kinase inhibitory effects of pyrimidinylpyrazole derivatives terminating with arylsulfonamido or cyclic sulfamide substituents. *Journal of enzyme inhibition and medicinal chemistry, 31*(sup2), 111–122. https://doi.org/10.1080/14756366.2016.1190715

[14] [Xing, Q., Jiang, D., Zhang, J., Guan, L., Li, T., Zhao, Y., Zhu, Z. (2022). Combining visible-light induction and copper catalysis for chemo-selective nitrene transfer for late-stage amination of natural products. *Communications Chemistry, 5*(1), 79. https://doi.org/10.1038/s42004-022-00692-6

[15] Davydenko, Y. M., Demeshko, S., Pavlenko, V. A., Dechert, S., Meyer, F., Fritsky, I. O. (2013). Synthesis, crystal structure, spectroscopic and magnetically study of two copper (II) complexes with pyrazole ligand. *Zeitschrift für anorganische und allgemeine Chemie, 639*(8-9), 1472-1476. https://doi.org/10.1002/zaac.201300078

[16] Cañón-Mancisidor, W., Hermosilla-Ibáñez, P., Spodine, E., Paredes-García, V., Gómez-García, C. J., Venegas-Yazigi, D. (2023). Spin Frustrated Pyrazolato Triangular CuII Complex: Structure and Magnetic Properties, an Overview. *Magnetochemistry, 9*(6), 155. https://doi.org/10.3390/magnetochemistry9060155

[17] Davydenko, Y., Pavlenko, V., Fritsky, I., Vynohradov, O. (2022). Synthesis, x-ray crystal structure, spectroscopic characterization and hirshfeld surface analysis of dichloro-bis (3,5-dimethyl-4-amino-1h-pyrazole) cobalt (II). *Ukrainian Chemistry Journal, 88*(6), 127–136. https://doi.org/10.33609/2708-129X.88.06.2022.127-136

[18] Mandal, N. K., Nandi, S., Souilamas, S. B., Garcia, C. J. G., Acharya, K., Naskar, J. P. (2024). Design, synthesis and structure of a trinuclear copper (II) complex having Cu_3OH core with regard to aspects of antiproliferative activity and magnetic properties. *New Journal of Chemistry*. https://doi.org/10.1039/D3NJ04859D

[19] Watanabe, Y., Washer, B. M., Zeller, M., Savikhin, S., Slipchenko, L. V., Wei, A. (2022). Copper (I)–Pyrazolate Complexes as Solid-State Phosphors: Deep-Blue Emission through a Remote Steric Effect. *Journal of the American Chemical Society, 144*(23), 10186–10192. https://doi.org/10.1021/jacs.1c13462

[20] Shi, K., Mathivathanan, L., Boudalis, A. K., Turek, P., Chakraborty, I., Raptis, R. G. (2019). Nitrite Reduction by Trinuclear Copper Pyrazolate Complexes: An Example

of a Catalytic, Synthetic Polynuclear NO Releasing System. *Inorganic Chemistry, 58*(11), 7537–7544. https://doi.org/10.1021/acs.inorgchem.9b00748

[21] Bagnarelli, L., Dolmella, A., Santini, C., Vallesi, R., Giacomantonio, R., Gabrielli, S., Pellei, M. (2021). A new dimeric Copper (II) complex of hexyl bis (pyrazolyl) acetate ligand as an efficient catalyst for allylic oxidations. *Molecules, 26*(20), 6271. https://doi.org/10.3390/molecules26206271

[22] Titi, A., Zaidi, K., Alzahrani, A. Y., El Kodadi, M., Yousfi, E. B., Moliterni, A., Abboud, M. (2023). New in situ catalysts based on nitro functional pyrazole derivatives and copper (II) salts for promoting oxidation of catechol to o-quinone. *Catalysts, 13*(1), 162. https://doi.org/10.3390/catal13010162

[23] You, P. Y., Mo, K. M., Wang, Y. M., Gao, Q., Lin, X. C., Lin, J. T., Li, D. (2024). Reversible modulation of interlayer stacking in 2D copper-organic frameworks for tailoring porosity and photocatalytic activity. *Nature Communications, 15*(1), 194. https://doi.org/10.1038/s41467-023-44552-w

[24] Shi, K., Mathivathanan, L., Herchel, R., Boudalis, A. K., Raptis, R. G. (2020). Supramolecular Assemblies of Trinuclear Copper (II)-Pyrazolato Units: A Structural, Magnetic and EPR Study. *Chemistry, 2*(3), 626–644. https://doi.org/10.3390/chemistry2030039

[25] Davydenko, Y. M., Vynohradov, O. S., Pavlenko, V. O., Fesych, I. V., Fritsky, I. O., Naumova, D. D., Shova, S. (2024). [Synthesis and crystal structure of Copper (II) 9-Azametallacrowns-3 with 4-iodopyrazole]. *Journal of Chemistry and Technologies, 32*(3), 554–569. (in Ukrainian). https://doi.org/10.15421/jchemtech.v32i3.305413

[26] Vynohradov, O. S., Davydenko, Y. M., Pavlenko, V. O., Naumova, D. D., Fritsky, I. O., Shova, S., Prysiazhna, O. V. (2023). $CuBr_2$ as a bromination agent of pyrazole-based ligand: synthesis of copper (II) coordination compounds by oxidative dissolution of copper powder in organic solvents. *Journal of Chemistry and Technologies, 31*(3), 493–506. https://doi.org/10.15421/jchemtech.v31i3.281190

[27] Davydenko, Y. M., Vitske, V. A., Pavlenko, V. A., Haukka, M., Vynohradov, O. S., Fritsky, I. O. (2022). Synthesis, crystal structure and properties of coordination polymers based on (3, 5-dimethyl-1H-pyrazole-4-yl)-acetic acid. Journal of Chemistry and Technologies, 30(2), 174–183. https://doi.org/10.15421/jchemtech.v30i2.252517

[28] Mukherjee, R. (2000). Coordination chemistry with pyrazole-based chelating ligands: molecular structural aspects. *Coordination Chemistry Reviews, 203*(1), 151–218. http://dx.doi.org/10.1016/S0010-8545(99)00144-7

[29] Senko, M. W. IsoPro Isotopic Abundance Simulator, v. 2.1; National High Magnetic Field Laboratory, Los Alamos National Laboratory: Los Alamos, NM, 1994.

[30] *CrysAlis PRO* 1.171.43.144a (Rigaku OD, 2024), SHELXT 2018/2 (Sheldrick, 2018), *SHELXL* 2018/3 (Sheldrick, 2015), Olex2 1.5-ac6-020 (Dolomanov *et al.*, 2009).

[31] Groom, C. R., Bruno, I. J., Lightfoot, M. P., Ward, S. C. (2016). The Cambridge structural database. Structural Science, 72(2), 171–179.

[32] Nakamoto, K. (2009). *Infrared and Raman Spectra of Inorganic and Coordination Compounds*. Hoboken, New Jersey: John Wiley&Sons.

[33] Chow, Y. M., Britton, D. O. Y. L. E. (1975). The crystal structures of dimethylthallium cyanide, azide, cyanate, and thiocyanate. *Structural Science*, *31*(7), 1922–1929. https://doi.org/10.1107/S0567740875006486

[34] Mezei, G., Zaleski, C. M., Pecoraro, V. L. (2007). Structural and functional evolution of metallacrowns. *Chemical reviews*, *107*(11), 4933–5003. https://doi:10.1021/cr078200h

[35] Addison, A. W., Rao, N. T., Reedijk, J., van Rijn, J., Verschoor, G. C. (1984). Synthesis, structure, and spectroscopic properties of copper(II) compounds containing nitrogen–sulphur donor ligands; the crystal and molecular structure of aqua[1,7-bis(N-methylbenzimidazol-2′-yl)-2,6-dithiaheptane]copper(II) perchlorate. *J. Chem. Soc., Dalton Trans.* 1349–1356. https://doi:10.1039/dt9840001349.

[36] Yang, L., Powell, D. R., Houser, R. P. (2007). Structural variation in copper(I) complexes with pyridylmethylamide ligands: structural analysis with a new four-coordinate geometry index, τ4. *Dalton Trans.* (9), 955–64. https://doi:10.1039/b617136b. PMID 17308676

[37] Spackman, P. R., Turner, M. J., McKinnon, J. J., Wolff, S. K., Grimwood, D. J., Jayatilaka, D., Spackman, M. A. (2021). CrystalExplorer: a program for Hirshfeld surface analysis, visualization and quantitative analysis of molecular crystals. *Applied Crystallography*, *54*(3), 1006–1011.